Earth and Planetary Science Letters 412 (2015) 163–172

Contents lists available at ScienceDirect

Earth and Planetary Science Letters

www.elsevier.com/locate/epsl

Tectonic activity as a significant source of crustal tetrafluoromethane emissions to the atmosphere: Observations in groundwaters along the San Andreas Fault

Daniel A. Deeds [a,*], Justin T. Kulongoski [a], Jens Mühle [b], Ray F. Weiss [b]

[a] California Water Science Center, United States Geological Survey, San Diego, CA, United States
[b] Scripps Institution of Oceanography, University of California, San Diego, CA, United States

ARTICLE INFO

Article history:
Received 10 June 2014
Received in revised form 5 December 2014
Accepted 9 December 2014
Available online 7 January 2015
Editor: G.M. Henderson

Keywords:
tetrafluoromethane
tectonic emissions
San Andreas Fault
crustal weathering
groundwater

ABSTRACT

Tetrafluoromethane (CF_4) concentrations were measured in 14 groundwater samples from the Cuyama Valley, Mil Potrero and Cuddy Valley aquifers along the Big Bend section of the San Andreas Fault System (SAFS) in California to assess whether tectonic activity in this region is a significant source of crustal CF_4 to the atmosphere. Dissolved CF_4 concentrations in all groundwater samples but one were elevated with respect to estimated recharge concentrations including entrainment of excess air during recharge (C_{re}; ~30 fmol kg^{-1} H_2O), indicating subsurface addition of CF_4 to these groundwaters. Groundwaters in the Cuyama Valley contain small CF_4 excesses (0.1–9 times C_{re}), which may be attributed to an *in situ* release from weathering and a minor addition of deep crustal CF_4 introduced to the shallow groundwater through nearby faults. CF_4 excesses in groundwaters within 200 m of the SAFS are larger (10–980 times C_{re}) and indicate the presence of a deep crustal flux of CF_4 that is likely associated with the physical alteration of silicate minerals in the shear zone of the SAFS. Extrapolating CF_4 flux rates observed in this study to the full extent of the SAFS (1300 km × 20–100 km) suggests that the SAFS potentially emits (0.3–1) × 10^{-1} kg CF_4 yr^{-1} to the Earth's surface. For comparison, the chemical weathering of ~7.5 × 10^4 km^2 of granitic rock in California is estimated to release (0.019–3.2) × 10^{-1} kg CF_4 yr^{-1}. Tectonic activity is likely an important, and potentially the dominant, driver of natural emissions of CF_4 to the atmosphere. Variations in preindustrial atmospheric CF_4 as observed in paleo-archives such as ice cores may therefore represent changes in both continental weathering and tectonic activity, including changes driven by variations in continental ice cover during glacial–interglacial transitions.

© 2014 Elsevier B.V. All rights reserved.

1. Introduction

Tetrafluoromethane (CF_4) is a long-lived and potent greenhouse gas (Cicerone, 1979; Ravishankara et al., 1993; Morris et al., 1995), with an estimated atmospheric lifetime of at least 50,000 years (Ravishankara et al., 1993) and a 100-year Global Warming Potential of 7390 CO_2-equivalents (Forster et al., 2007). The global atmospheric abundance of CF_4 has more than doubled in the past half-century due to anthropogenic emissions (Worton et al., 2007; Mühle et al., 2010). CF_4 is naturally present in accessory fluorites in granitic rocks in the continental crust (Harnisch et al., 1996, 2000; Harnisch and Eisenhauer, 1998); the release of terrigenic CF_4 from continental weathering has sustained a measurable natural atmospheric background prior to industrial emissions (Harnisch et al., 1996; Worton et al., 2007; Mühle et al., 2010). Emissions of terrigenic CF_4 to the atmosphere are still poorly constrained, but have been associated with continental rather than oceanic crust (Harnisch et al., 1996; Deeds et al., 2008a; 2008b), and particularly with weathering of granitic alluvium and with crustal tectonic processes (Deeds et al., 2008b).

The weathering of silicate minerals in the continental crust, coupled with carbonate burial in the oceans, constitutes a major sink of atmospheric carbon dioxide on geologic timescales (Berner et al., 1983). The rate of chemical weathering of continental rocks depends on temperature, precipitation runoff, and the atmospheric CO_2 mole fraction (Amiotte Suchet and Probst, 2003; Gislason et al., 2009). Recent research suggests that chemical weathering rates are particularly sensitive to changes in atmospheric CO_2 and global climate, with a modeled 50% increase in chemical weathering rates resulting from a doubling of atmospheric CO_2 (Beaulieu et al., 2012). Large changes in atmospheric CO_2 throughout the Phanerozoic (541 Myr BP – present) coincide

* Corresponding author.
E-mail address: ddeeds@usgs.gov (D.A. Deeds).

http://dx.doi.org/10.1016/j.epsl.2014.12.016
0012-821X/© 2014 Elsevier B.V. All rights reserved.

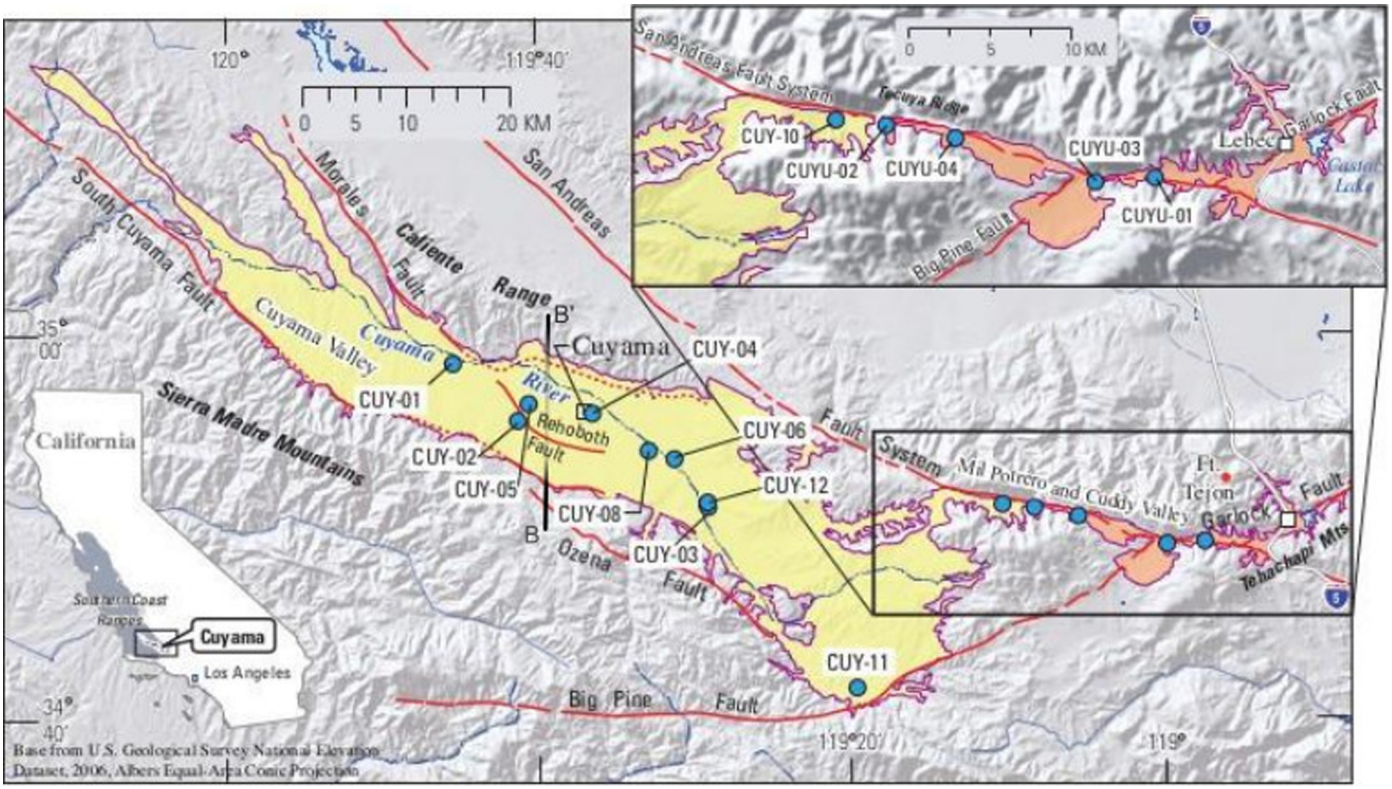

Fig. 1. Map of the Cuyama, Mil Potrero and Cuddy Valleys along the Big Bend section of the San Andreas Fault System in California, USA. The location of major faults, geographic features and wells sampled in this study are shown.

with changes in global silicate weathering (Goudie and Viles, 2012 and references therein). Hence, understanding the links between continental weathering, atmospheric CO_2 and global climate may aid in forecasting the response of weathering to future changes in atmospheric CO_2.

As natural CF_4 is closely associated with felsic rocks in the continental crust and has a natural atmospheric residence time on the order of 100,000 years (Ravishankara et al., 1993; Morris et al., 1995; Deeds et al., 2008b), changes in the paleo-atmospheric CF_4 record may provide insight into the response of chemical weathering to changes in atmospheric CO_2 on timescales of thousands of years or more. For example, ancient air in Greenland ice core samples dating from 11 to 19 kyr BP was found to contain 34.66 ± 0.16 ppt CF_4 (Mühle et al., 2010). In comparison, preindustrial (160–40 yr BP) air in ice core samples from an alpine ice core and from Greenland and Antarctic firn contained 39 ± 6 ppt CF_4 (Harnisch et al., 1996), 34 ± 1 ppt (Worton et al., 2007) and 34.90 ± 0.04 ppt (Mühle et al., 2010), respectively, which suggests that crustal weathering has been steady from the Last Glacial Maximum to the present. Measurements of CF_4 over 800 kyr in the Dome C ice core record show small variability in atmospheric CF_4 mole fractions (31–35 ppt) with higher CF_4 during interglacials and lower CF_4 during glacials (Schmitt et al., 2013). In addition, the authors observed a shift towards higher atmospheric CF_4 after 430 kyr BP and a sharp increase in atmospheric CF_4 during Marine Isotope Stage 11 (424–374 kyr BP), which they proposed were due to changes in crustal weathering (Schmitt et al., 2013).

Inferring changes in continental weathering from past atmospheric CF_4 abundances assumes there are no other mechanisms for the release of terrigenic CF_4 to the atmosphere. However, elevated CF_4 concentrations in groundwaters near active faulting in Southern California suggest that tectonics may play a role in crustal degassing of CF_4 (Deeds et al., 2008b), potentially complicating the use of CF_4 as a paleo-weathering proxy. Further studies would help improve our understanding of the release mechanisms of terrigenic CF_4 and the interplay between continental weathering, atmospheric CO_2 mixing ratios and global climate.

In this study, we report dissolved CF_4 concentrations measured in groundwaters from several aquifers along the Big Bend section of the San Andreas Fault System in the Southern Coast Range of California. We estimate the terrigenic CF_4 contributions to these concentrations by accounting for anthropogenic additions to these samples, assess the mechanisms of release CF_4 release in this region, and consider whether tectonic activity along the San Andreas Fault System is a significant driver of crustal CF_4 degassing to the atmosphere.

2. Study area description

Groundwater samples were collected from aquifers in the Cuyama, Mil Potrero and Cuddy Valleys (Fig. 1). The study area lies within the seismically-active San Andreas Fault System (SAFS) which, in this region, is dominated by northwest-trending, right-lateral strike-slip faults. The Cuyama Valley is bounded to the north by the Morales fault and to the west and south by the South Cuyama, Ozena and Big Pine faults, all of which are associated with the SAFS (Kulongoski et al., 2013). The primary water-bearing formations are mainly unconsolidated fluvial and alluvial deposits of <500 m thickness in Cuyama Valley (Fig. 2) (Sweetkind et al., 2013) and 100–150 m thickness in the Mil Potrero and Cuddy Valleys (CDWR, 2004). Water-bearing deposits are composed of Holocene-age (<11.7 kyr BP) granitic alluvium (alternating layers of sands, gravels, silts and clays) and Pleistocene-age (2.6 Myr–11.7 kyr BP) terrestrial deposits (poorly-consolidated arkosic sands, silts, clays and gravels) (Mathany et al., 2009). Cuyama Valley water-bearing deposits overlie a roughly 1100–3800 m thick sequence of Pliocene-age (5.3–2.6 Myr BP) non-marine and Oligocene to Miocene-age (33.9–5.3 Myr BP) marine sandstones and claystones (Sweetkind et al., 2013). The Mesozoic-age (252–66 Myr BP)

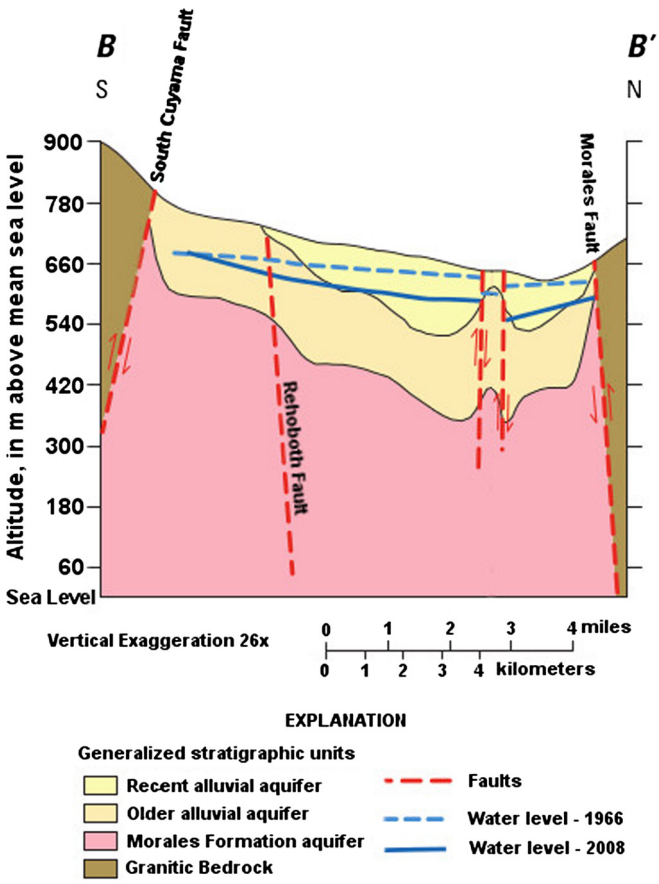

Fig. 2. A geologic cross-section of the shallow Cuyama Valley (modified from Sweetkind et al., 2013). Young fluvial and older alluvial water-bearing deposits overlie a thick section of low-yield mixed marine–non-marine sandstones/claystones (Morales Formation). The crystalline basement is not encountered at depths shown in the cross-section.

granitic basement underlying Cuyama deposits has been encountered near wells Cuy-06 and Cuy-11 at depths of roughly 4000 and 1200 m below land surface, respectively. In all other locations the marine sandstones are underlain by pre-Oligocene deposits of undetermined depth (Sweetkind et al., 2013).

In contrast to the Cuyama Valley, the Mil Potrero and Cuddy Valley deposits are relatively thin (<150 m) and are underlain either directly by the Mesozoic-age granitic/gneissic crystalline basement or by a roughly 1000 m thick Miocene-age sequence of poorly-sorted claystone, sandstone and conglomerate (CDWR, 2004; Kulongoski et al., 2013). The study area is bounded on the west and south by the Sierra Madre Mountains, on the south by Mount Pinos, Cerro Noroeste and Sawmill Mountain, on the north by the Caliente Range and Tecuya Ridge, and on the east by the Tehachapi Mountains. The surrounding mountains are comprised mainly of Mesozoic granites, volcanics and sedimentary units (Sweetkind et al., 2013).

3. Methods

Groundwater samples for trace gas analyses were collected from nine wells in the Cuyama Valley and from five wells in Mil Potrero and Cuddy Valley aquifers. Wells in this study are 24 cm or 36 cm diameter production wells equipped with electric turbine pumps. Inactive wells were purged with 3 or more borehole-casing volumes prior to sampling. Two liters of groundwater were collected into an evacuated 2.5 L glass flask with a flow-through stopcock to limit intrusion of ambient air into collected samples. Several meters of Tygon tubing attached to the outflow of the stopcock allowed the sampling team to collect whole water samples (including degassed bubbles if present) without entrainment of external air. A single sample was collected at each well. Samples were shipped and stored in the laboratory at ∼20 °C for several weeks prior to analysis by cryo-trapping of exsolved gases into an evacuated cold finger cooled with liquid helium (Deeds et al., 2008b). Exsolved gases were then passed through a 30.5 cm-length, 6.3 mm-diameter Ascarite II (sodium hydroxide coated silica) pre-column for carbon dioxide removal prior to preconcentration, gas chromatographic separation and mass spectrometric detection with a "Medusa" GC-MS (Miller et al., 2008). The full details of the analysis can be found in Deeds et al. (2008b) and Miller et al. (2008). Blank-corrected mole fractions of analytes were determined by comparison to whole-air standards on the SIO-2005 calibration scale (Prinn et al., 2000), and were converted to molal concentrations using the measured sample water mass. Measured CF_4 concentrations, as well as concentrations of chlorofluorocarbons CFC-12 (CCl_2F_2), CFC-11 (CCl_3F) and CFC-113 ($C_2Cl_3F_3$), are presented in Table 1. The Medusa GC-MS instrumentation used in this study regularly measures the analytes presented in Table 1 with precisions of 0.05–1.5% (Miller et al., 2008). The uncertainties of CF_4, CFC-12, CFC-11 and CFC-113 measurements in this study are estimated at ±4%, ±5%, ±7% and ±5%, respectively, with the majority of error arising from uncertainties in blank corrections and propagation of measurement errors (±2–3%), and from uncertainty associated with correcting for incomplete extraction of analytes from collected groundwater samples (±2–5%). CF_4 and CFC measurements of duplicate groundwater samples tend to agree to within ±5% (Deeds et al., 2008b).

The Medusa GC-MS measures sulfur hexafluoride (SF_6), another long-lived greenhouse gas that is also present in granitic rock (Harnisch and Eisenhauer, 1998). The modern atmospheric abundance of SF_6 is at least three orders of magnitude larger than the pre-industrial atmospheric background (Maiss and Brenninkmeijer, 1998; Vollmer and Weiss, 2002) leading to easily discernible modern signals in recently recharged groundwater (Busenberg and Plummer, 2000). However, SF_6 was undetectable in several Cuddy Valley groundwater samples with CFC concentrations that are consistent with a large contribution of recent recharge. We also note that xenon, which elutes from the Medusa's GC with a similar retention time to SF_6 and has an air-saturated water concentration (∼10^{-8} cc STP g^{-1} water Krause and Benson, 1989) that would under standard operating conditions produce a small response in the Medusa GC-MS, was not observed in extracted gases in Mil Potrero and Cuddy Valley groundwaters where SF_6 concentrations were below detection limits. Based on this evidence and on the inspection of recorded pressure and flow-rate data collected during Medusa GC-MS measurement, we propose that the carbon dioxide present in samples was not completely removed by the Ascarite II precolumn, and that excess CO_2 collected on the cryotraps of the Medusa GC-MS resulted in breakthrough and loss of high volatility analytes (e.g. SF_6 and Xe) during the preconcentration steps of the analysis. For this study, we consider SF_6 results to be compromised and unsuitable for use in interpreting our results.

The Medusa GC-MS uses two cryotraps to separate CF_4 from other analytes with minimal co-transfer of CO_2 and other bulk gases. Past experiments have shown that the Medusa GC-MS successfully recovers CF_4 from whole-air CF_4 standards with elevated CO_2 mole fractions (Miller et al., 2008). If CF_4 were lost to incomplete trapping then reported concentrations and fluxes in this study would need to be considered as lower limits to actual values.

4. Results and discussion

Dissolved CF_4 in groundwater originates from both the atmosphere and lithosphere (Fig. 3). We use major and minor ion con-

Table 1
Depth of top (ToP) and bottom (BoP) of well perforation (in m below land surface), apparent radiocarbon age ($\tau_{^{14}C}$, in kyr) (Mathany et al., 2009), tritium concentration (^3H, in TU) [21], measured CFC concentrations (in pmol kg^{-1} H_2O), the fraction modern groundwater in a sample (f), the modern groundwater CFC age (τ_{CFC}), ambient air contamination (A_c) estimated from CFC concentrations, and the measured (meas) and excess (ex) CF_4 concentrations for Cuyama Valley and Mil Potrero/Cuddy Valley groundwaters (collected during the Groundwater Ambient Monitoring and Assessment (GAMA) campaign).

GAMA ID	ToP (m b.l.s.)	BoP (m b.l.s.)	$\tau_{^{14}C}$ (kyr)	^3H (TU)	CFC-11 (CCl_3F)	CFC-12 (CCl_2F_2)	CFC-113 ($C_2Cl_3F_3$)	f	τ_{CFC} (yr)	A_c (mmol kg^{-1} H_2O)	$[CF_4]_{meas}$	$[CF_4]_{ex}$[a]
					(pmol kg^{-1} H_2O)						(fmol kg^{-1} H_2O)	
Cuyama Valley groundwaters												
Cuy-01	14	38	2.6	0.90	1.45	1.13	0.131	0.26	18	0.02	54	37
Cuy-02	104	241	33.4	<0.1	0.0824	0.191	0.033	0	–	0.33	131	105
Cuy-03	N/A	N/A	0.60	2.2	14.8	15.1	0.654	1	<15	0.01	82	9
Cuy-04	128	219	3.6	0.28	0.248	0.276	0.045	0.89	48	0.04	38	2
Cuy-05	N/A	N/A	25.8	<0.1	0.133	0.276	0.044	0	–	0.50	3.7×10^2	3.3×10^2
Cuy-06	195	244	1.2	2.1	55.1	4.04	0.255	1	23	0.01	36	11
Cuy-08	N/A	187[b]	2.5	2.8	0.945	0.565	0.050	1	40	0.01	25	3
Cuy-11	N/A	N/A	3.5	0.78	1.17	1.96	0.118	0.20	16	0.03	55	36
Cuy-12	N/A	32[b]	1.1	2.0	138	3.97	0.404	1	21	0.01	85	32
Mil Potrero/Cuddy Valley groundwaters												
Cuy-10	44	88	1.1	0.87	0.814	1.01	0.067	0.15	20	0.02	1.73×10^4	1.73×10^4
Cuyu-01	12	59	0.54	2.3	3.89	2.78	0.478	1	20	0.38	2.4×10^2	2.4×10^3
Cuyu-02	16	78	2.1	2.6	4.14	2.47	0.407	1	22	0.08	69	38
Cuyu-03	N/A	72[b]	0.24	2.1	4.77	2.85	0.494	1	<15	0.03	6.9×10^2	6.2×10^2
Cuyu-04	N/A	N/A	1.7	1.4	2.26	1.29	0.119	0.45	<15	0.01	72	48

[a] CF_4 excess, calculated as $([CF_4]_M - f \times [CF_4]_{R,Y} - (1-f) \times [CF_4]_{R,O} - A_c * Z_{2008})$ where $[CF_4]_M$, f, $[CF_4]_{R,Y}$ and $[CF_4]_{R,O}$ are defined in Fig. 3, A_c is the modern air contamination concentration and Z_{2008} is the 2008 atmospheric CF_4 mole fraction.
[b] Perforation depth not available, well depth given in place of bottom of perforation.

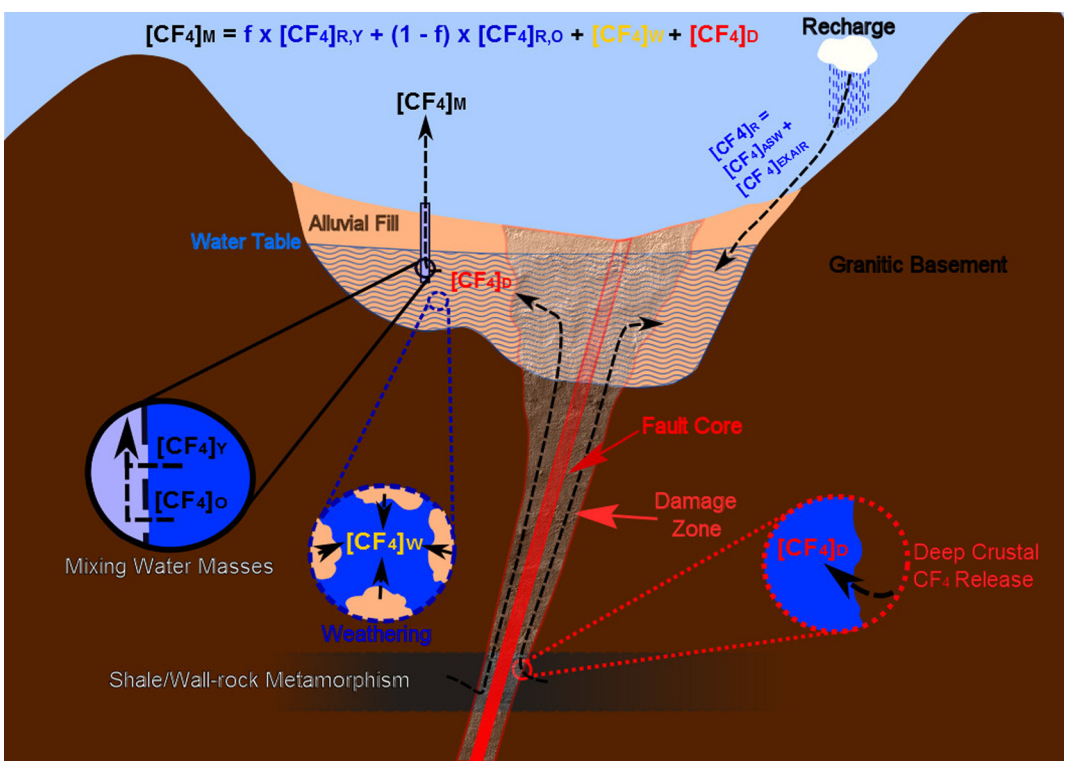

Fig. 3. Schematic illustration of atmospheric and lithospheric CF_4 inputs to an idealized granitic aquifer. CF_4 concentrations in recharge ($[CF_4]_R$) are estimated from recharge altitude and temperature and measured neon concentrations (Kulongoski et al., 2013). Recharge concentrations are elevated above air-saturated water concentrations ($[CF_4]_{ASW}$) due to air-entrainment ($[CF_4]_{EXAIR}$). Groundwater samples are often a mixture of young and old groundwaters, with a CF_4 concentration that can be represented by a two-end member mixing model: $[CF_4]_M = f \times [CF_4]_Y + (1-f) \times [CF_4]_O$, where f is the fraction of young groundwater present, estimated using measured CFC concentrations. Within the aquifer, groundwater accumulates terrigenic CF_4 from weathering of surrounding granitic alluvium ($[CF_4]_W$) constrained using the NETPATH chemical mass balance model (Plummer et al., 1991) and available major and minor ion concentrations. The contribution of deep crustal CF_4 ($[CF_4]_D$) is taken as the residual in $[CF_4]_M$ after accounting for all other CF_4 inputs to collected groundwaters.

centrations, isotopic tracers and noble gas concentrations, collected as part of the Groundwater Ambient Monitoring and Assessment (GAMA) project (see Mathany et al., 2009 for details) to constrain atmospheric and lithospheric inputs, as described in the following sections, to better understand the role the SAFS plays in facilitating terrigenic CF_4 emissions to the Earth's surface.

4.1. Modern contributions of CF_4 to collected samples

Production wells often sample from a wide depth range, drawing a mixture of deep older waters and shallow recently-recharged waters (Fig. 3). In the lithosphere, the weathering of silicate minerals and transfer of CF_4 to groundwater occurs on timescales of thousands of years (Deeds et al., 2008b) with CF_4 accumulating in ancient, deeper groundwaters. However, recently recharged groundwaters contain anthropogenic atmospheric CF_4, which must be accounted for in order to estimate the terrigenic CF_4 concentrations in groundwater samples. The proportion of young, recently recharged groundwater in a sample, and the age of recent recharge, can be constrained by comparing the partial pressure of chlorofluorocarbons (CFCs) in equilibrium with the sample to atmospheric CFC histories (Plummer and Busenberg, 2000), as CFCs are solely anthropogenic in origin and were introduced into the environment in the mid-20th century (Butler et al., 1999). If we assume that the young groundwater component in a sample is not itself a mixture of water masses, then the young groundwater's contribution to a mixed-age sample (f) can be estimated from the ratio of the measured equilibrium CFC partial pressure ($p_{CFC_{eq}}$) to the respective atmospheric partial pressures at the time of recharge (τ), $p_{CFC}(\tau)$. Equilibrium $p_{CFC_{eq}}$ are estimated from measured CFC concentrations using the estimated altitude and temperature of recharge and corresponding solubility constants, and the entrainment of excess air during recharge and ambient air during sampling or analysis are accounted for and subtracted, as discussed below. The ratio of partial pressures of two CFCs in a groundwater mixture is insensitive to dilution with CFC-free pre-industrial groundwater, and may be used to constrain the time of recharge, but may be altered by (bio-) degradation under reducing conditions (Plummer and Busenberg, 2000). Cuyama groundwater samples were classified as either oxic ($n = 13$) or mixed (oxic–anoxic, $n = 3$) based on available dissolved oxygen, NO_3, Mn, Fe, SO_4 and H_2S concentrations (McMahon and Chapelle, 2008; NWIS, 2012). Comparison of p_{cfc} ratios in equilibrium with a collected sample to atmospheric CFC histories should therefore provide a reliable estimate of the apparent age (τ) of recent recharge in a sample (Plummer and Busenberg, 2000).

Recharge to the Cuyama Valley aquifers occurs predominately via the Cuyama River (CDWR, 2004). In this study, monthly streamflow data from 1960 to 2008 (NWIS, 2012) and mean air temperatures in the Cuyama valley from 1944 to 2008 (WRCC, 2013) were used to construct a time-series of annual recharge temperatures. Altitude for recharge is set at 750 m, the median surface altitude of wells sampled in Cuyama Valley, with a median absolute deviation (MAD) of 80 m. Recharge to the Mil Potrero and Cuddy Valley aquifers occurs as mountain-front recharge (CDWR, 2004), and recharge temperature is thus taken from neighboring mountain temperature records (WRCC, 2013). We adopt the median recharge altitude of 1580 m, with an MAD of 60 m, previously estimated for Mil Potrero and Cuddy Valley groundwaters (Kulongoski et al., 2013). Variability in estimated recharge altitude on the order of tens of meters should contribute to a minor increase in uncertainty in CFC air-saturated water concentrations (Darling et al., 2012). Annual average atmospheric CFC mole fractions are estimated from air measurements at Trinidad Head, California (Prinn et al., 2000). Regional atmospheric CFC mole fractions may be elevated by fugitive emissions from nearby urban centers (Gentner et al., 2010), and as such the estimated CFC age of recent recharge may be biased young (e.g. ~6 years for observed CFC-11 mole fractions recently observed downwind of Los Angeles, Gentner et al., 2010). However, the overestimation of modern CF_4 present in samples is likely small (~15% for the example above) (Mühle et al., 2010). Estimated partial pressures of CFCs in a groundwater sample are corrected for addition of CFCs in excess air entrained during recharge (Aeschbach-Hertig et al., 2000). Excess air concentrations are estimated from measured neon concentrations (Kulongoski et al., 2013) and range from 0.03 to 0.77 mmol kg^{-1} H_2O. Excess air CFC corrections are scaled by the fraction of young water in a sample, f, as pre-industrial excess air will contain neon but is not expected to contain CFCs.

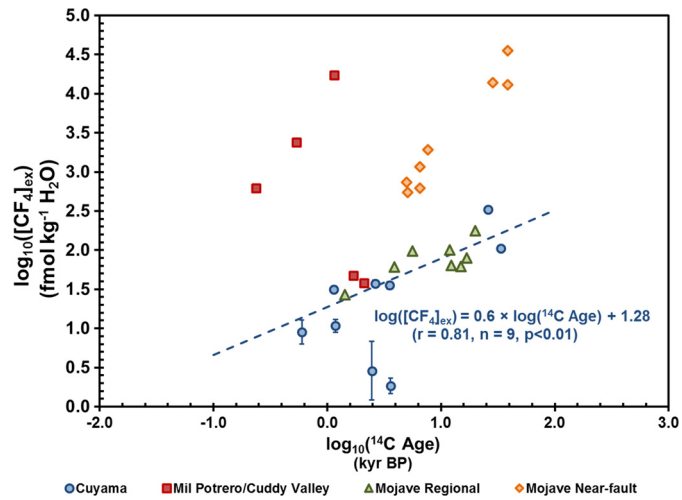

Fig. 4. Excess CF_4 concentrations plotted against apparent radiocarbon ages for the Cuyama and Mil Potrero/Cuddy Valley aquifers. Radiocarbon ages are calculated using a half-life of 5568 years and are uncorrected for carbonate chemistry. Regional Mojave Desert groundwaters ("Regional") and Mojave Desert groundwaters located near faults in the Eastern Californian Shear Zone ("Near-fault") from Deeds et al. (2008a) are also plotted for comparison. The plotted error-weighted regression includes only Cuyama Valley groundwaters.

Samples from two wells drawing pre-nuclear (i.e. ^3H-free) groundwater (Cuy-02 and Cuy-05) contain small concentrations of CFCs in molar ratios consistent with air contamination, added either during sampling or analysis, equivalent to the addition of 0.3–0.5 mmol air per kg^{-1} H_2O. For the remainder of groundwater samples, we included an ambient air contamination term (A_c) that was allowed to vary between 0–5 mmol kg^{-1} H_2O in increments of 0.01 mmol kg^{-1} H_2O until CFC residuals were minimized. Ambient air contributions estimated in this manner ranged from 0.01 to 0.5 mmol air kg^{-1} H_2O (<3% of estimated dissolved air concentrations in samples, median of 0.03 mmol kg^{-1} H_2O), of similar range to estimates from previous studies using the same methodology (Deeds et al., 2008a; 2008b). The resulting f, A_C and τ estimates for each well are presented in Table 1. Seven wells contain CFC concentrations consistent with 100% modern groundwater, with CFC ages ranging from <15 to 40 years. The remaining seven samples contain a modern water component ranging from 0% (pre-industrial groundwater) to 89% (median of 26%), with CFC ages of <15 to 48 years where datable. Although groundwater samples collected contain significant proportions of recently recharged groundwater, modern CF_4 only accounts for on average 40% of measured CF_4 concentrations. The uncertainty of excess CF_4 concentrations (i.e. corrected for modern contributions) varies by well but has a median value of ±10%.

4.2. The origin of terrigenic CF_4 in Cuyama Valley groundwaters

There is a gradual accumulation of CF_4 in Cuyama Valley groundwaters over thousands of years (Fig. 4) that closely resembles the growth of CF_4 excesses observed in regional Mojave Desert groundwaters located in the Eastern Californian Shear Zone (ECSZ) (Deeds et al., 2008b). This may reflect similarities in climate and geology between the two regions. Precipitation in the Cuyama Valley and the Mojave Desert is low, and recharge to the aquifers is highly localized, with groundwater entering chiefly

through the upper reaches of ephemeral streams and rivers and through mountain-front recharge (Izbicki et al., 2000). The water-bearing units in the Cuyama Valley and Mojave Desert aquifers are thick (>500 m) sections of late Pliocene- to Pleistocene-age deposits derived from pre-Tertiary-age crystalline and metamorphic rocks in the surrounding mountains (Riley and Worts, 1953; CDWR, 1967; Sweetkind et al., 2013). However, in the Mil Potrero and Cuddy valleys, groundwaters often contain large excesses of CF_4 that are inconsistent with their estimated radiocarbon ages (Fig. 4). Given previous evidence for tectonic emissions of CF_4 (Deeds et al., 2008b) the San Andreas Fault is the hypothesized source of excess CF_4 in nearby groundwaters.

To assess the tectonic flux of CF_4 through the SAFS we first account for *in situ* release of terrigenic CF_4 from weathering of the surrounding granitic deposits (Fig. 3). In the Mojave Desert regional aquifer the accumulation of terrigenic CF_4 was attributed mainly to *in situ* release due to weathering of the aquifer material (Deeds et al., 2008b). The accumulation of excess CF_4 in Cuyama groundwaters, comparable to Mojave groundwaters, suggests that Cuyama Valley groundwaters might be useful for constraining the weathering flux of CF_4 to Mil Potrero and Cuddy Valley groundwaters, and thus the SAFS-related flux. To this end, we estimate primary silicate weathering in the Cuyama Valley using the mass balance model NETPATH (Plummer et al., 1991), accounting for carbonate precipitation/dissolution, cation exchange and incongruent primary silicate dissolution to clay (e.g. kaolinite or montmorillonite). The source rock for Cuyama Valley water-bearing deposits is the granitic Salinian block in nearby mountains, which is composed primarily of granodiorite and quartz monzonite (Jennings et al., 1977). Primary silicate weathering was therefore modeled as dissolution of oligoclase and plagioclase with 30% anorthite. Silica, calcium, sodium and magnesium concentrations (NWIS, 2012) were used as constraints, with hydrochemical data from the upper reaches of the Cuyama River used to set initial conditions for the evolution of sampled Cuyama groundwaters (CCRWQCB, 2011; NWIS, 2012). Weathering estimates therefore include dissolution during recharge through the unsaturated zone of the aquifer. The mass of silicate dissolved by Cuyama groundwaters ($m_{silicate}$) per kilogram of groundwater is estimated to be (0.15–2.2) × 10^2 mg kg^{-1} H_2O, with an average of 86 mg kg^{-1} H_2O (Table 2). The contribution of weathering to measured CF_4 concentrations in Cuyama groundwaters ($[CF_4]_W$) can then be estimated from:

$$[CF_4]_W = m_{silicate} \times \zeta_r$$

where ζ_r is the CF_4 mass ratio in granites. If we assume a median granitic CF_4 mass ratio of 12 ppt (parts-per-trillion, median absolute deviation [MAD] of 10 ppt) (Harnisch and Eisenhauer, 1998; Harnisch et al., 2000), then primary silicate dissolution contributes (0.2–3) × 10^1 fmol of CF_4 to Cuyama Valley groundwaters (Table 2). The contribution of primary silicate dissolution to measured CF_4 excesses ranges from 7 to 390% (median of 29%), suggesting that chemical weathering is generally insufficient to supply the observed CF_4 excesses in Cuyama groundwaters.

The current dataset of crustal CF_4 content is derived primarily from European granites with limited spatial coverage elsewhere (Harnisch and Eisenhauer, 1998; Harnisch et al., 2000). It is possible that the estimated weathering flux of CF_4 is low due to an underestimation of the CF_4 content of the surrounding deposits. If the CF_4 content of Cuyama granite is assumed to equal the median CF_4 content of North American granite, 39 ppt ($n = 5$, MAD of 37 ppt) (Harnisch and Eisenhauer, 1998; Harnisch et al., 2000), then the weathering release of CF_4 to Cuyama groundwaters would account for 21–1280% (median of 94%) of measured CF_4 concentrations. If we adopt the maximum North American CF_4 content of 265 ppt (Harnisch and Eisenhauer, 1998,Harnisch et al., 2000), then CF_4 contributions from weathering are consistently overestimated, accounting for 1.5–87 times the measured CF_4 excesses in Cuyama groundwaters.

Table 2
Primary Silicate Dissolution (PSD) and deep crustal CF_4 ($[CF_4]_D$) corrected for contributions from weathering of the surrounding aquifer rock ($[CF_4]_W$).

GAMA ID	PSD (g silicate kg^{-1} H_2O)	$[CF_4]_W$ (fmol CF_4 kg^{-1} H_2O)	$[CF_4]_D$ (fmol CF_4 kg^{-1} H_2O)
Cuyama Valley groundwaters			
Cuy-01	0.10	14	36
Cuy-02	0.22	30	75
Cuy-03	0.018	2.4	6.5
Cuy-04	0.053	7.2	−5.4
Cuy-05	0.21	29	3.0×10^2
Cuy-06	0.023	3.1	7.7
Cuy-08	0.024	3.3	−0.4
Cuy-11	0.10	13.6	31
Cuy-12	0.015	2.1	30
Mil Potrero/Cuddy Valley groundwaters[*]			
Cuy-10	–	3.4	1.73×10^4
Cuyu-01	–	1.1	2.4×10^3
Cuyu-02	–	4.2	34
Cuyu-03	–	0.5	6.2×10^2
Cuyu-04	–	3.4	45

[*] Estimated from median weathering CF_4 flux in Cuyama groundwaters (see main text for details).

We note that the range of measured CF_4 content in North American granites (1.8–265 ppt) effectively covers the global range of measured granitic CF_4 content (1–265 ppt), which might indicate that the higher median CF_4 content in North American granites is an artifact of the relatively sparse sampling of this subset of the full dataset. The distribution of CF_4 content in granites is highly skewed towards values of <20 ppt (Supplementary Fig. S1), arguing for adoption of a low CF_4 content for granites of unknown composition. In the absence of statistical evidence to distinguish the CF_4 content of North American granites from the global distribution we therefore use the global median granitic CF_4 content to estimate the weathering CF_4 flux from water-bearing deposits in Cuyama Valley.

Excess CF_4 concentrations, corrected for CF_4 release from weathering of surrounding granitic deposits (i.e. $[CF_4]_D = [CF_4]_{meas} - [CF_4]_W$), are plotted as a function of distance to the nearest fault in Fig. 5. The weathering contribution to CF_4 excesses in Mil Potrero and Cuddy Valley groundwaters was estimated using their measured radiocarbon ages and the median weathering CF_4 flux for Cuyama Valley groundwaters (2.3 fmol CF_4 kg^{-1} H_2O kyr^{-1}, Tables 1, 2). Young groundwater (datable with ^3H–^3He) has been shown to rapidly accumulate perfluorinated gases (SF_6) (von Rohden et al., 2010), with the rate of accumulation slowing for older groundwater (datable with ^{14}C) (Deeds et al., 2008b; von Rohden et al., 2010). It is possible that $[CF_4]_W$ estimates in Table 2 for Mil Potrero and Cuddy Valley groundwaters are underestimated by adopting a $[CF_4]_W$ flux based on older Cuyama Valley groundwaters, although relatively young Cuyama groundwaters (e.g. Cuy-03) contain $[CF_4]_W$ concentrations of comparable magnitude to $[CF_4]_W$ estimates for Mil Potrero and Cuddy Valley groundwaters.

The highest CF_4 excesses in the Mil Potrero and Cuddy Valley groundwaters are found within 200 m of the San Andreas Fault suggesting a deep source of CF_4 associated with fluids migrating through the fault zone. Geophysical studies have identified a low-velocity damage zone (i.e. highly fractured rock) around the SAFS that extends from the surface down to seismogenic depths with an estimated width of 150–200 m (Li et al., 2004; Zoback et al., 2010). The CF_4 findings presented in this study are consistent with fluid migration through the permeable deposits

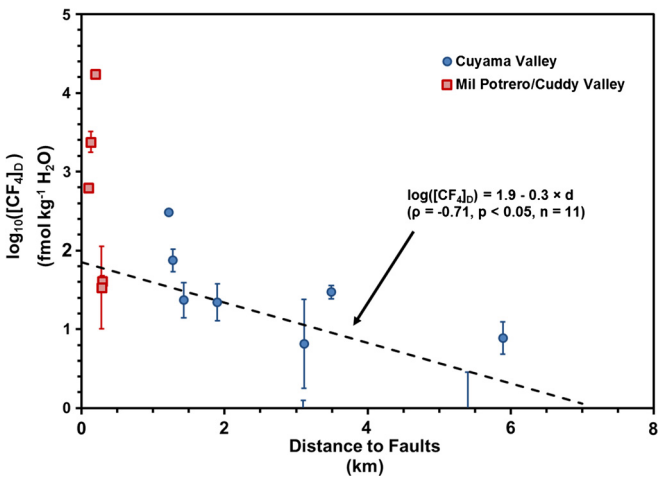

Fig. 5. Deep crustal CF_4 ($[CF_4]_D$) (Fig. 3) plotted against distance to the nearest fault, calculated as $[CF_4]_D = [CF_4]_{ex} - [CF_4]_W$, where $[CF_4]_W$ is the weathering CF_4 release and $[CF_4]_{ex}$ is total CF_4 excess. For Mil Potrero and Cuddy Valley groundwaters, the nearest fault is the San Andreas. The nearest faults for most Cuyama Valley groundwaters are either the surrounding faults delimiting the extent of the groundwater basin or the Rehoboth Fault (Fig. 1). Groundwater samples with negative $[CF_4]_D$ (Cuy-04 and Cuy-08) are plotted as error bars only.

in the fractured zone surrounding the fault core (Wiersberg and Erzinger, 2008).

Wells further than 200 m from the SAFS typically also contain residual terrigenic CF_4, which is significantly anti-correlated with distance to nearby faults (Spearman's rho $\rho = -0.71$, $n = 11$, $p < 0.05$) (Fig. 5), providing evidence for a flux of CF_4 through faults associated with the SAFS. Assuming the median CF_4 excess found within 200 m of the San Andreas Fault, 2.3×10^3 fmol kg^{-1} H_2O, represents the initial fluid entering the extended system of faults associated with the San Andreas Fault System, we then estimate that 0–13% of Cuyama Valley groundwaters originate from SAFS fluids migrating through associated faults. Helium isotope ratios suggest that deeply sourced fluids are a minor component (0–6%) to Cuyama Valley groundwaters (Kulongoski et al., 2013), broadly consistent with fault fluid contributions estimated using residual terrigenic CF_4. Discrepancies from the general trend in Fig. 5 may be due to uncertain distances to local faulting (e.g. Cuy-05) or to significant recharge along the Cuyama River (e.g. Cuy-04).

Carbon dioxide and helium concentrations and carbon and helium isotope systematics in Mil Potrero and Cuddy Valley groundwaters (Kulongoski et al., 2013), and at the San Andreas Fault Observatory at Depth (SAFOD) drill site (Wiersberg and Erzinger, 2011), indicate that deeply sourced fluids in the San Andreas Fault originate primarily from metamorphism of organic-rich shales and carbonates at depth (~3 km below land surface Wiersberg and Erzinger, 2011), with a smaller contribution from mantle fluids entering the fault from below. Measurements of the CF_4 content in metamorphic rock are limited and do not include shales (Harnisch and Eisenhauer, 1998; Harnisch et al., 2000). Busenberg and Plummer (2000) detected low concentrations of SF_6 in a sample of marine carbonate. Concentrations of CF_4 in deep Pacific seawater suggest that CF_4 is not associated with the oceanic lithosphere (Deeds et al., 2008a), which may argue against CF_4 being present in marine carbonates, but seawater for CF_4 measurement was collected at an open ocean site distant from continental shelves and associated marine carbonate deposits. No evidence has been found to date for a mantle source of CF_4 (Jordan et al., 2000; Frische et al., 2006; Deeds et al., 2008a). Rock cuttings from the SAFOD borehole show a high degree of low temperature alteration associated with fluid–rock interaction (Schleicher et al., 2009), suggesting that deeply sourced CF_4 may originate in water–rock interaction between the granitic wall rock and fluids migrating to the surface.

Geochemical comparisons of wall rock and fault rock fragments indicate that 17–58% of wall rock mass is lost to stress-driven dissolution in the SAFS (Schleicher et al., 2009). Silica mass balances for fault rocks require fluid–rock ratios of $(0.5–1.4) \times 10^2$ mL fluid per g rock in the deep SAFS (Schleicher et al., 2009), which when combined with estimated mass losses gives an estimated 10^{-2}–10^1 g rock dissolved kg^{-1} fluid. If we assume a CF_4 content of 12 ppt (Harnisch and Eisenhauer, 1998; Harnisch et al., 2000) for wall rocks of the SAFS, then deep fluid–rock interaction in the SAFS could contribute 10^3–10^6 fmol CF_4 kg^{-1} fluid to vertically migrating fluids. This estimate is inherently uncertain given the lack of CF_4 measurements in deep crustal rocks and therefore shows only that fluid–rock interaction has the potential to supply the high CF_4 excesses observed in close proximity to the San Andreas Fault. It may also be possible that fracturing of wall rock caused by transient fluid overpressuring during slip events (Mittempergher et al., 2011) releases CF_4 into fluids migrating through the SAFS.

4.3. CF_4 fluxes through the San Andreas Fault: implications for crustal CF_4 degassing

If the excess CF_4 observed in Big Bend groundwaters originates predominately from the SAFS then it is possible that tectonic forcing represents an important mechanism for degassing terrigenic CF_4. In Sections 4.3 and 4.4 we assess CF_4 emissions to the atmosphere from the SAFS and global tectonics, respectively. Although the calculations in these sections often rely on assumptions regarding understudied aspects of CF_4 geochemistry and on extrapolations from small (aquifer) to large (continental/global) spatial scales, they illustrate the potential that tectonics play in controlling the preindustrial atmospheric CF_4 abundance.

Excess CF_4 concentrations in Big Bend groundwaters can be combined with vertical fluid flow rates for the SAFS to estimate the potential flux of CF_4 through the entire SAFS to the Earth's surface ($F_{CF_4,fault}$, in fmol m^{-2} yr^{-1}):

$$F_{CF4,fault} = [CF_4]_D \times \rho_{H_2O} \times F_{fluid}$$

where $[CF_4]_D$ is the observed CF_4 excess in groundwaters along the SAFS, corrected for weathering, in fmol kg^{-1} H_2O, ρ_{H_2O} is the density of water (~10^3 kg m^3) and F_{fluid} is the vertical fluid flow rate, in m yr^{-1}. The vertical flow rate through the Big Bend section of the SAFS is at least 0.147 m yr^{-1}, based on measured helium concentrations and helium isotope ratios in Mil Potrero and Cuddy Valley groundwaters (Kulongoski et al., 2013). However, helium concentrations and helium isotope ratios in well fluids and springs at Parkfield, CA, ~130 km to the northwest of Cuyama Valley, indicate a much lower rate of fluid migration through the SAFS, 0.003 m yr^{-1} (Kennedy et al., 1997). Excess CF_4 concentrations in Cuyama Valley, Mil Potrero and Cuddy Valley groundwaters appear to be consistent with both a high vertical fluid flow focused near to the main trace of the San Andreas Fault and a more diffuse flux of fluid through faults associated with the SAFS. If we assume a vertical fluid flow rate of 0.147 m yr^{-1} for the main trace of the San Andreas Fault and an effective fluid flow rate of 3 mm yr^{-1} for the extended SAFS, and assume that the median CF_4 excess of 2.4×10^3 fmol CF_4 kg^{-1} H_2O within 200 m of the San Andreas Fault represents SAFS fault fluids, then the CF_4 flux through the main trace of the SAFS would be 3.5×10^5 fmol CF_4 m^{-2} yr^{-1} and the CF_4 flux through the extended SAFS would be 7×10^3 fmol CF_4 m^{-2} yr^{-1}. For reference, the basal flux of CF_4 entering Mojave Desert groundwaters through local fault systems was previously estimated to be $(0.2–5) \times 10^4$ fmol CF_4 m^{-2} yr^{-1} (Deeds et al., 2008b), which is of comparable magnitude to the flux estimate derived above for the extended SAFS.

The dimensions of the SAFS have been estimated to be 1300 km length × 100 km width (Wallace, 1990). Helium and carbon dioxide measurements in Big Bend groundwaters suggest that emissions are confined to a narrower width of approximately 20 km (Kulongoski et al., 2013). As a first estimate we assume CF_4 emissions observed along the SAFS in the Big Bend represent emissions throughout the full length and width of the SAFS; further studies at other locations along the SAFS would refine the estimates in this study. The total flux of CF_4 through the SAFS can be estimated from:

$$F_{CF_4,tot} = (L_{SAFS} \times w_{main}) \times F_{CF_4,main} + \left(L_{SAFS} \times (w_{ext} - w_{main})\right) \times F_{CF_4,ext}$$

where L_{SAFS} is the length of the SAFS (1300 km), w is the width of the main trace (400 m) and the extended (ext) SAFS (20–100 km) and F_{CF_4} is the corresponding flux through the respective regions. With a focused flux of 3.5×10^5 fmol CF_4 $m^{-2}\,yr^{-1}$ along the main trace of the SAFS and a flux of 7×10^3 fmol CF_4 $m^{-2}\,yr^{-1}$ out to 10–50 km distance, the total annual flux of CF_4 through the SAFS is estimated to be $(0.3–1) \times 10^{-1}$ kg CF_4 yr^{-1}. The main trace of the SAFS contributes between 16 and 50% of the total annual flux of CF_4, depending on the width adopted for the extended system of faults associated with the SAFS.

One may assess the geologic relevance of deeply-sourced CF_4 emissions through the SAFS by considering the potential quantity of CF_4 available in the damage zone for release into fault fluids. Taking a damage zone width of 200 m, an SAFS length of 1300 km and assuming CF_4 release is confined to the roughly 300 m zone of metamorphism encountered at ∼3 km depth in the SAFS (Wiersberg and Erzinger, 2011) (Fig. 3), then approximately 7.8×10^{10} m^3 of CF_4-containing rock may be available along the main trace of the SAFS. Using a density of 2.7 $g\,cm^{-3}$ for granites, and a CF_4 content of 12 ppt (by mass), the main trace of the SAFS potentially has 2.5×10^6 g CF_4 available for release. We estimate in the previous paragraph a flux of 0.016 kg CF_4 kyr^{-1} through the main trace of the fault, which suggests that the SAFS contains sufficient CF_4 to sustain the observed flux for roughly 160 Myr.

To put the flux of CF_4 through the SAFS into a regional context we estimate CF_4 emissions associated with the weathering of granites across California. The emissions of CF_4 associated with a weathering of a granitic surface (W, in $g\,yr^{-1}$) can be estimated from:

$$W = C_s \times SA_g \times MW_g \times [CF_4]$$

where C_s is the specific annual consumption of granitic rocks (in mol granite $km^{-2}\,yr^{-1}$), SA_g is the area of the granitic surface (in km^2), MW_g is the molecular weight of granite (in $g\,mol^{-1}$) and $[CF_4]$ is the granitic CF_4 mass content (in g CF_4 g^{-1} granite). The specific annual consumption of granitic rocks (modeled as albite) by weathering has been estimated to be 40.36×10^3 mol silicate $km^{-2}\,yr^{-1}$ (equivalent to a denudation rate of 0.04 $mm\,yr^{-1}$) (Amiotte Suchet and Probst, 2003). Granitic rock and metamorphic rocks derived from granites (e.g. gneiss) cover 18% of the roughly 4.1×10^5 km^2 surface area of California (Jennings et al., 1977). Allowing the granitic CF_4 mass content to vary over the full range previously measured, 1–265 ppt (Harnisch and Eisenhauer, 1998; Harnisch et al., 2000), and assuming a molecular mass of 263.02 $g\,mol^{-1}$ granite (i.e. MW_{albite}), we estimate that chemical weathering of Californian granites might release $(0.08–2.2) \times 10^{-2}$ kg CF_4 yr^{-1} to the atmosphere. This estimate does not include chemical weathering of the 1.4×10^5 km^2 of alluvial and glacial deposits across California (Jennings et al., 1977) that may contain granitic rock and thus terrigenic CF_4. If we assume that Californian glacial sediments and alluvium contain the same range of CF_4 content as granites and assume a specific annual consumption rate of 30.92×10^3 mol sediments $km^{-2}\,yr^{-1}$ (Amiotte Suchet and Probst, 2003), then chemical weathering of these deposits may release up to an additional $(0.011–3.0) \times 10^{-1}$ kg CF_4 yr^{-1} to the atmosphere. The total potential terrigenic CF_4 weathering flux across California would then be $(0.019–3.2) \times 10^{-1}$ kg CF_4 yr^{-1}. Metamorphism associated with the tectonic forcing of the SAFS is therefore a significant, and possibly the dominant, release mechanism for terrigenic CF_4 present in the California crust. However, on a global scale, the $(0.3–1) \times 10^{-1}$ kg CF_4 yr^{-1} flux of CF_4 through the SAFS would be a small contributor to the $(2–5) \times 10^3$ kg CF_4 yr^{-1} necessary (Harnisch and Eisenhauer, 1998) to maintain the observed preindustrial atmospheric background of roughly 34 ppt CF_4 (Harnisch et al., 1996; Worton et al., 2007; Mühle et al., 2010) with a preindustrial atmospheric lifetime of 110–280 kyr (Ravishankara et al., 1993; Morris et al., 1995).

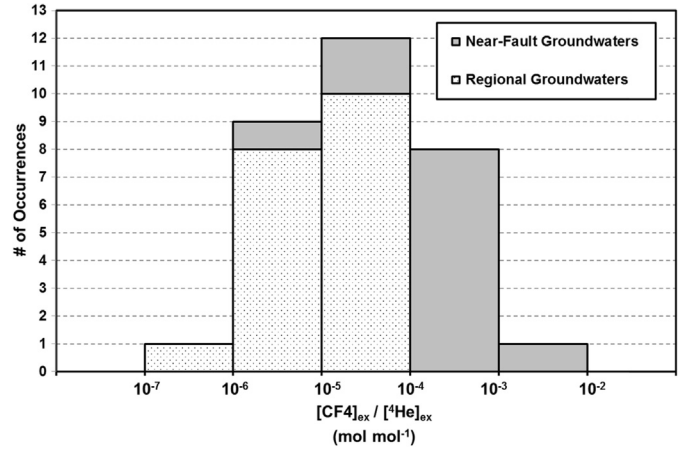

Fig. 6. Histogram of the molar ratio of terrigenic CF_4 to crustal helium-4 for regional groundwaters and near-fault groundwaters in the Eastern California Shear Zone (Deeds et al., 2008b; Kulongoski et al., 2003, 2005, 2013) and along the San Andreas Fault (this study).

4.4. Extrapolating global CF_4 fluxes associated with tectonic activity via $CF_4/^4He$ ratios in groundwater

Deeds et al. (2008b) estimated a global lithospheric flux of $(0.8–4) \times 10^3$ kg CF_4 yr^{-1} by analogy to the global crustal degassing of helium (Torgersen and O'Donnell, 1991; Ballentine and Burnard, 2002) and by using Mojave Desert $CF_4/^4He$ molar ratios of $(0.3–1.5) \times 10^{-4}$ mol CF_4 (mol^{-1} He) based on the hypothesis that crustal He degassing is controlled mainly by tectonically-driven hydrofracture and enhanced vertical fluid migration in regions of crustal extension such as the ECSZ (Torgersen and O'Donnell, 1991; Ballentine and Burnard, 2002; Kulongoski et al., 2005). The histogram of $CF_4/^4He$ molar ratios from the combined dataset of this study and the Mojave Desert (Deeds et al., 2008b; Kulongoski et al., 2003, 2005, 2013) (Fig. 6) shows a log-normal distribution of $CF_4/^4He$ molar ratios in groundwater between 10^{-6}–10^{-3}, with a median value of 2.1×10^{-5} (MAD of 1.7×10^{-5}).

There appears to be a distinct geochemical signal in the $CF_4/^4He$ ratio for regional groundwaters versus groundwaters in proximity to faulting (Fig. 6). This may reflect preferential release of He over larger, heavier gases from aquifer rock in low temperature environments such as shallow groundwaters (Ballentine et al., 1994) versus enhanced release of both gases during hydrofracture and higher temperature metamorphism in the fault zone at depth (Torgersen and O'Donnell, 1991). The molar $CF_4/^4He$ in fault fluids may therefore more accurately reflect crustal $CF_4/^4He$ ratios but the regional $CF_4/^4He$ ratio is likely more representative of the diffuse crustal flux throughout regions of crustal extension

and deformation. If we assume that the inner 50% of "regional" $CF_4/^4He$ molar ratios, $(0.4–2.2) \times 10^{-5}$, represents the global diffuse flux of CF_4 associated with tectonic activity, and assume a helium flux of 3×10^8 moles He yr^{-1} from granites in the crust (Deeds et al., 2008b), then the global tectonic flux of CF_4 is estimated to be $(1.1–5.8) \times 10^2$ kg CF_4 yr^{-1}. For comparison assuming a global coverage of 37.13×10^6 km^2 for shield rocks and 35.42×10^6 km^2 for sands and sandstones, and corresponding weathering rates of 40.36×10^3 and 30.92×10^3 moles km^{-2} yr^{-1}, respectively (Amiotte Suchet and Probst, 2003), and assuming a range of 1–265 ppt CF_4 in granites (Harnisch and Eisenhauer, 1998; Harnisch et al., 2000) then the global flux of CF_4 associated with chemical weathering of the crust is $(0.007–1.8) \times 10^2$ kg CF_4 yr^{-1}. The total crustal degassing flux in this study, $(0.11–0.76) \times 10^3$ kg, is consistent with the previous crustal CF_4 flux estimate (weathering plus metamorphism) of $(0.1–1) \times 10^3$ kg CF_4 yr^{-1} (Harnisch and Eisenhauer, 1998). Further study of the CF_4 content of the continents and measurement of the flux of terrigenic CF_4 through fault zones other than the SAFS would help further refine the weathering and tectonic CF_4 emissions estimates presented here. At present the findings of this study suggest that crustal extension and deformation associated with tectonics has the potential to be as significant a release mechanism for crustal CF_4 as chemical weathering. Historical changes in the pre-industrial atmospheric CF_4 abundance may therefore be driven in part by other processes than the chemical weathering of the crust, and any future interpretation of paleo-atmospheric CF_4 as a weathering proxy must be approached with caution.

5. Conclusion

CF_4 concentrations were measured in groundwaters from wells in the Cuyama Valley, Mil Potrero and Cuddy Valley basins along the San Andreas Fault. All but one groundwater sample contained CF_4 in excess of modern air-saturated water concentration, providing evidence for a lithospheric source of CF_4 to shallow groundwater systems. Cuyama Valley groundwater CF_4 excesses increase gradually with groundwater age, at a rate similar to the *in situ* weathering flux observed in the nearby Mojave Desert. After accounting for weathering input of CF_4 to Cuyama Valley groundwaters, residual CF_4 excesses associated with the faults that delineate the valley floor were identified. Groundwaters in the Mil Potrero and Cuddy Valley basins located within 200 m of the San Andreas Fault contain CF_4 excesses that are several orders of magnitude higher than elsewhere in the region, suggesting the presence of a deep crustal flux associated with fluids migrating vertically through the fault. The flux of CF_4 extrapolated to the full length and width of the SAFS is comparable in magnitude to chemical weathering releases for California as a whole. Extrapolating further to the global scale, tectonic metamorphism is likely an important mechanism for the release of natural crustal CF_4 to the atmosphere and thus for sustaining pre-industrial atmospheric CF_4 abundances on millennial and longer timescales.

Acknowledgements

The authors thank the cooperating well owners and water purveyors for allowing access to wells for sampling. Funding was provided by the United States Geological Survey California Water Science Center, California State bonds administered by the State Water Resources Control Board Groundwater Ambient Monitoring and Assessment Program, and in part by the AGAGE program under NASA grant NAG5-12807. This manuscript benefited greatly from the comments of K. Haase and 2 anonymous reviewers.

Appendix A. Supplementary material

Supplementary material related to this article can be found online at http://dx.doi.org/10.1016/j.epsl.2014.12.016.

References

Aeschbach-Hertig, W., Peeters, F., Beyerle, U., Kipfer, R., 2000. Palaeotemperature reconstruction from noble gases in ground water taking in to account equilibration with entrapped air. Nature 405, 1040–1044. http://dx.doi.org/10.1038/35016542.

Amiotte Suchet, P., Probst, J.L., 2003. A global model for present day atmospheric/soil CO_2 consumption by chemical erosion of continental rocks (GEM-CO2). Tellus, Ser. B Chem. Phys. Meteorol. 47, 273–280. http://dx.doi.org/10.1034/j.1600-0889.47.issue1.23.x.

Ballentine, C.J., Mazurek, M., Gautschi, A., 1994. Thermal constraints on crustal rare gas release and migration: evidence from Alpine fluid inclusions. Geochim. Cosmochim. Acta 58, 4333–4348. http://dx.doi.org/10.1016/0016-7037(94)90337-9.

Ballentine, C.J., Burnard, P., 2002. Production of noble gases in the continental crust. In: Porcelli, D., Ballentine, C.J., Wieler, R. (Eds.), Noble Gases in Geochemistry and Cosmochemistry, vol. 47. Mineral. Soc. Am., Washington, DC, pp. 481–538.

Beaulieu, E., Goddéris, Y., Donnadieu, Y., Labat, D., Roelandt, C., 2012. High sensitivity of the CO_2 sink by continental weathering to the future climate change. Nat. Clim. Change 2, 346–349. http://dx.doi.org/10.1038/nclimate1419.

Berner, R.A., Lasaga, A.C., Garrels, R.M., 1983. The carbonate–silicate geochemical cycle and its effect on atmospheric carbon dioxide over the past 100 million years. Am. J. Sci. 283, 641–683.

Busenberg, E., Plummer, L.N., 2000. Dating young groundwater with sulfur hexafluoride: natural and anthropogenic sources of sulfur hexafluoride. Water Resour. Res. 36, 3011–3030. http://dx.doi.org/10.1029/2000WR900151.

Butler, J.H., Battle, M., Bender, M., Montzka, S.A., Clarke, A.D., Saltzman, E.S., Sucher, C., Severinghaus, J., Elkins, J.W., 1999. A twentieth century record of atmospheric halocarbons in polar firn air. Nature 399, 749–765. http://dx.doi.org/10.1038/21586.

California Department of Water Resources (CDWR), 1967. Mojave River groundwater basin investigation. Bull.-Calif., Dep. Water Resour. 84.

California Department of Water Resources (CDWR), 2004. California Ground Water Bulletin 118. Accessed November 2011 online at http://www.water.ca.gov/groundwater/bulletin118/gwbasin_maps_descriptions.cfm.

Central Coast Regional Water Quality Control Board (CCRWQCB), 2011. Central Coast Ambient Monitoring Program Data Navigator. Accessed November 2011 at http://www.ccamp.org.

Cicerone, R.J., 1979. Atmospheric carbon tetrafluoride: a nearly inert gas. Science 206, 59–61. http://dx.doi.org/10.1126/science.206.4414.59.

Darling, W.G., Gooddy, D.C., MacDonald, A.M., Morris, B.L., 2012. The practicalities of using CFCs and SF6 for groundwater dating and tracing. Appl. Geochem. 27, 1688–1697. http://dx.doi.org/10.1016/j.apgeochem.2012.02.005.

Deeds, D.A., Mühle, J., Weiss, R.F., 2008a. Tetrafluoromethane in the deep North Pacific Ocean. Geophys. Res. Lett. 35, L14606. http://dx.doi.org/10.1029/2008GL034355.

Deeds, D.A., Vollmer, M.K., Kulongoski, J.T., Miller, B.R., Mühle, J., Harth, C.M., Izbicki, J.A., Hilton, D.R., Weiss, R.F., 2008b. Evidence for crustal degassing of CF_4 and SF_6 in Mojave Desert groundwaters. Geochim. Cosmochim. Acta 72, 999–1013. http://dx.doi.org/10.1016/j.gca.2007.11.027.

Forster, P., Ramaswamy, V., Artaxo, P., Berntsen, T., Betts, R., Fahey, D.W., Haywood, J., Lean, J., Lowe, D.C., Myhre, G., Nganga, J., Prinn, R., Raga, G., Schulz, M., Dorland, R.V., 2007. Changes in atmospheric constituents and in radiative forcing. In: Solomon, S., Qin, D., Manning, M., Chen, Z., Marquis, M., Averyt, K.B., Tignor, M., Miller, H.L. (Eds.), Climate Change 2007: The Physical Science Basis. Contribution of Working Group I to the Fourth Assessment Report of the Intergovernmental Panel on Climate Change. Cambridge University Press, Cambridge, United Kingdom and New York, NY, USA.

Frische, M., Garofalo, K., Hansteen, T.H., Borchers, R., Harnisch, J., 2006. The origin of stable halogenated compounds in volcanic gases. Environ. Sci. Pollut. Res. 13, 406–413. http://dx.doi.org/10.1065/espr2006.01.291.

Gentner, D.R., Miller, A.M., Goldstein, A.H., 2010. Seasonal variability in anthropogenic halocarbon emissions. Environ. Sci. Technol. 44, 5377–5382. http://dx.doi.org/10.1021/es1005362.

Gislason, S.R., Oelkers, E.J., Eiriksdottir, E.S., Kardjilov, M.I., Gisladottir, G., Sigfusson, B., Snorrason, A., Elefsen, S., Hardardottir, J., Torssander, P., Oskarsson, N., 2009. Direct evidence of the feedback between climate and weathering. Earth Planet. Sci. Lett. 277, 213–222. http://dx.doi.org/10.1016/j.epsl.2008.10.018.

Goudie, A.S., Viles, H.A., 2012. Weathering and the global carbon cycle: geomorphological perspectives. Earth-Sci. Rev. 113, 59–71. http://dx.doi.org/10.1016/j.earscirev.2012.03.005.

Harnisch, J., Borchers, R., Fabian, P., Gäggeler, H.W., Schotterer, U., 1996. Effect of natural tetrafluoromethane. Nature 384, 32. http://dx.doi.org/10.1038/384032a0.

Harnisch, J., Eisenhauer, A., 1998. Natural CF_4 and SF_6 on Earth. Geophys. Res. Lett. 25, 2401–2404. http://dx.doi.org/10.1029/98GL01779.

Harnisch, J., Frische, M., Borchers, R., Eisenhauer, A., Jordan, A., 2000. Natural fluorinated organics in fluorite and rocks. Geophys. Res. Lett. 27, 1883–1886. http://dx.doi.org/10.1029/2000GL008488.

Izbicki, J.A., Radyk, J., Michel, R.L., 2000. Water movement through a thick unsaturated zone underlying an intermittent stream in the western Mojave Desert, southern California, USA. J. Hydrol. 238, 194–217. http://dx.doi.org/10.1016/S0022-1694(00)00331-0.

Jennings, C.W., Strand, R.G., Rogers, T.H., 1977. Geologic map of California. California Division of Mines and Geology. Scale 1:750,000.

Jordan, A., Harnisch, J., Borchers, R., Le Guern, F., Shinohara, H., 2000. Volcanogenic halocarbons. Environ. Sci. Technol. 34, 1122–1124. http://dx.doi.org/10.1021/es990838q.

Kennedy, B.M., Kharaka, Y.K., Evans, W.C., Ellwood, A., DePaolo, D.J., Thordsen, J., Ambats, G., Mariner, R.H., 1997. Mantle fluids in the San Andreas Fault system, California. Science 633, 1278–1281. http://dx.doi.org/10.1126/science.278.5341.1278.

Krause, D., Benson, B.B., 1989. The solubility and isotopic fractionization of gases in dilute aqueous solution IIa. Solubilities of the noble gases. J. Solution Chem. 18, 823–873. http://dx.doi.org/10.1007/BF00685062.

Kulongoski, J.T., Hilton, D.R., Izbicki, J.A., 2003. Helium isotope studies in the Mojave Desert, California: implications for groundwater chronology and regional seismicity. Chem. Geol. 202, 95–113. http://dx.doi.org/10.1016/j.chemgeo.2003.07.002.

Kulongoski, J.T., Hilton, D.R., Izbicki, J.A., 2005. Source and movement of helium in the Morongo groundwater basin: the influence of regional tectonics on crustal and mantle helium fluxes. Geochim. Cosmochim. Acta 69, 3857–3872. http://dx.doi.org/10.1016/j.gca.2005.03.001.

Kulongoski, J.T., Hilton, D.R., Barry, P.H., Esser, B.K., Hillegonds, D., Belitz, K., 2013. Volatile fluxes through the Big Bend section of the San Andreas Fault, California: helium and carbon dioxide systematics. Chem. Geol. 339, 92–102. http://dx.doi.org/10.1016/j.chemgeo.2012.09.007.

Li, Y.-G., Vidale, J.E., Cochran, E.S., 2004. Low-velocity damaged structure of the San Andreas Fault at Parkfield from fault zone trapped waves. Geophys. Res. Lett. 31, L12S06. http://dx.doi.org/10.1029/2003GL019044.

Maiss, M., Brenninkmeijer, C.A.M., 1998. Atmospheric SF6: trends, sources, and prospects. Environ. Sci. Technol. 32, 3077–3086. http://dx.doi.org/10.1021/es9802807.

Mathany, T.M., Kulongoski, J.T., Ray, M.C., Belitz, K., 2009. Groundwater quality data in the South Coast Interior Basins study unit, 2008: results from the California GAMA program. U.S. Geological Survey Data Series 463.

McMahon, P.B., Chapelle, F.H., 2008. Redox processes and water quality of selected principal aquifers. Ground Water 46, 259–271. http://dx.doi.org/10.1111/j.1745-6584.2007.00385.x.

Miller, B.R., Weiss, R.F., Salameh, P.K., Tanhua, T., Greally, B.R., Mühle, J., Simmonds, P., 2008. Medusa: a sample preconcentration and GC/MS detector system for in situ measurements of atmospheric trace halocarbons, hydrocarbons, and sulfur compounds. Anal. Chem. 80, 701536–701545. http://dx.doi.org/10.1021/ac702084k.

Mittempergher, S., Toro, G.D., Gratier, J.P., Hadizadeh, J., Smith, S., 2011. Evidence of transient increases of fluid pressure in SAFOD Phase III Cores. Geophys. Res. Lett. 38, L03301. http://dx.doi.org/10.1029/2010GL046129.

Morris, R.A., Miller, T.M., Viggiano, A.A., Paulson, J.F., Solomon, S., Reid, G., 1995. Effects of electron and ion reactions on atmospheric lifetimes of fully fluorinated compounds. J. Geophys. Res. 100 (D1), 1287–1294. http://dx.doi.org/10.1029/94JD02399.

Mühle, J., Ganesan, A.L., Miller, B.R., Salameh, P.K., Harth, C.M., Greally, B.R., Rigby, M., Porter, L.W., Steel, L.P., Trudinger, C.M., Krummel, P.B., O'Doherty, S., Fraser, P.J., Simmonds, P.G., Prinn, R.G., Weiss, R.F., 2010. Perfluorocarbons in the global atmosphere: tetrafluoromethane, hexafluoroethane and octafluoropropane. Atmos. Chem. Phys. 10, 5145–5164. http://dx.doi.org/10.5194/acp-10-5145-2010.

National Water Information System (NWIS), 2012. Accessed online November 2011 at http://waterdata.usgs.gov/nwis.

Plummer, L.N., Prestemon, E.C., Parkhurst, D.L., 1991. An interactive code (NETPATH) for modelling net geochemical reactions along a flow path. U.S. Geological Survey Water-Resources Investigations Report 94-4078.

Plummer, L.N., Busenberg, E., 2000. Chlorofluorocarbons. In: Environmental Tracers in Subsurface Hydrology. Kluwer Academic, Boston, pp. 441–478. Chapter 15.

Prinn, R.G., Weiss, R.F., Fraser, P.J., Simmonds, P.G., Cunnold, D.M., Alyea, F.N., O'Doherty, S., Salameh, P., Miller, B.R., Huang, J., Wang, R.H.J., Hartley, D.E., Harth, C., Steele, L.P., Sturrock, G., Midgley, P.M., McCulloch, A., 2000. A history of chemically and radiatively important gases in air deduced from ALE/GAGE/AGAGE. J. Geophys. Res. 105 (D14), 17751–17792. http://dx.doi.org/10.1029/2000JD900141.

Ravishankara, A.R., Solomon, S., Turnipseed, A.A., Warren, R.F., 1993. Atmospheric lifetimes of long-lived halogenated species. Science 259, 194–199. http://dx.doi.org/10.1126/science.259.5092.194.

Riley, F.S., Worts Jr., G.F., 1953. Geology and groundwater appraisal of the Twentynine Palms Marine Corps Training Center, CA. USGS Open File Report 98-617.

Schleicher, A.M., Tourscher, S.N., van der Pluijm, B.A., Warr, L.N., 2009. Constraints on mineralization, fluid–rock interaction, and mass transfer during faulting at 2–3 km depth from the SAFOD drill hole. J. Geophys. Res. 114. http://dx.doi.org/10.1029/2008JB006092.

Schmitt, J., Seth, B., Köhler, P., Willenbring, J., Fischer, H., 2013. CF_4 and CO_2-coupling weathering and carbon cycle. Mineral. Mag. 77, 2161. hdl:10013/epic.42365.

Sweetkind, D.S., Faunt, C.C., Hansen, R.T., 2013. Construction of 3-D geologic framework and textural models for Cuyama Valley groundwater basin. U.S. Geological Survey Scientific Investigations Report 2013-5127.

Torgersen, T., O'Donnell, J., 1991. The degassing flux from the solid earth: release by fracturing. Geophys. Res. Lett. 18, 951–954. http://dx.doi.org/10.1029/91GL00915.

Vollmer, M.K., Weiss, R.F., 2002. Simultaneous determination of sulfur hexafluoride and three chlorofluorocarbons in water and air. Mar. Chem. 78, 137–148. http://dx.doi.org/10.1016/S0304-4203(02)00015-4.

von Rohden, C., Kreuzer, A., Chen, Z., Aeschbach-Hertig, W., 2010. Accumulation of natural SF_6 in the sedimentary aquifers of the North China Plain as a restriction on groundwater dating. Isot. Environ. Health Stud. 46, 279–290. http://dx.doi.org/10.1080/10256016.2010.494771.

Wallace, R.E., 1990. The San Andreas Fault system, California. US Geological Survey Professional Paper, 1515.

Western Regional Climate Center (WRCC), 2013. Accessed online November 2011 at http://www.wrcc.dri.edu/.

Wiersberg, T., Erzinger, J., 2008. Origin and spatial distribution of gas at seismogenic depths of the San Andreas Fault from drill-mud gas analysis. Appl. Geochem. 23, 1675–1690. http://dx.doi.org/10.1016/j.apgeochem.2008.01.012.

Wiersberg, T., Erzinger, J., 2011. Chemical and isotope compositions of drilling mud gas from the San Andreas Fault Observatory at Depth (SAFOD) borehole: implications on gas migration and the permeability structure of the San Andreas Fault. Chem. Geol. 284, 148–159. http://dx.doi.org/10.1016/j.chemgeo.2011.02.016.

Worton, D.R., Sturges, W.T., Gohar, L.K., Shine, K.P., Martinerie, P., Oram, D.E., Humphrey, S.P., Begley, P., Gunn, L., Barnola, J.-M., Schwander, J., Mulvaney, R., 2007. Atmospheric trends and radiative forcings of CF_4 and C_2F_6 inferred from firn air. Environ. Sci. Technol. 41, 2184–2189. http://dx.doi.org/10.1021/es061710t.

Zoback, M.D., Hickman, S.H., Ellsworth, B., 2010. Scientific drilling into the San Andreas fault zone. Eos 91, 197–204. http://dx.doi.org/10.1029/2010EO220001.